iScience

Article

The zinc receptor, ZnR/GPR39, modulates taste sensitivity by regulating ion secretion in mouse salivary gland

Graphical abstract

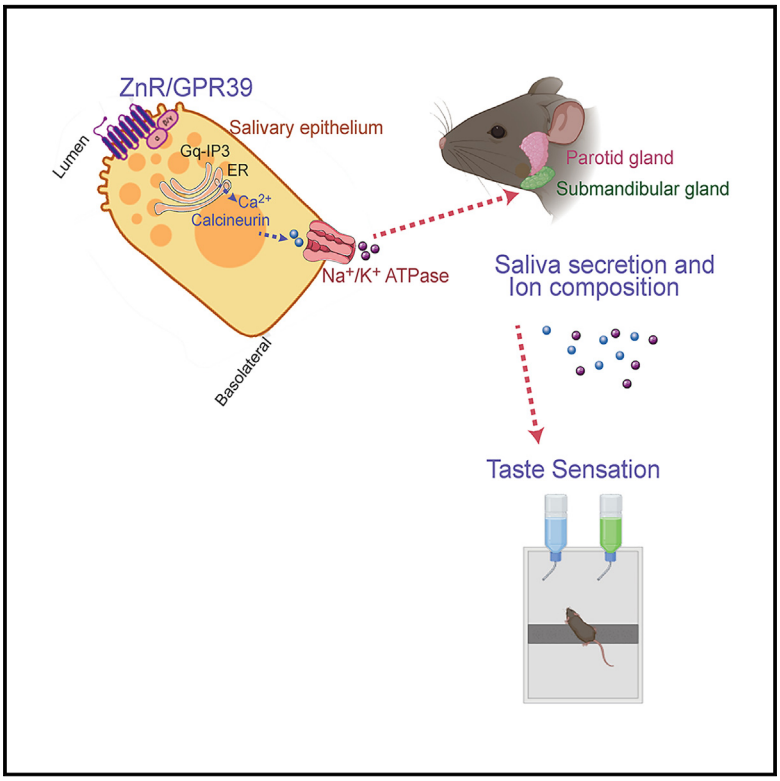

Authors

Moran Melamed, Hila Asraf, Noa Livne, ..., Avi Schroeder, Israel Sekler, Michal Hershfinkel

Correspondence

hmichal@bgu.ac.il

In brief

Natural sciences; Biological sciences; Biochemistry; Physiology

Highlights

- The zinc receptor, ZnR/GPR39, mediates zinc signaling in salivary gland
- ZnR/GPR39 regulates saliva composition and secretion
- ZnR/GPR39 controls the Na^+/K^+ ATPase activity in salivary epithelial cells
- Loss of ZnR/GPR39 activity impairs saliva secretion and salt taste sensation

Melamed et al., 2025, iScience *28*, 111912
February 21, 2025
https://doi.org/10.1016/j.isci.2025.111912

CellPress

iScience

CellPress
OPEN ACCESS

Article

The zinc receptor, ZnR/GPR39, modulates taste sensitivity by regulating ion secretion in mouse salivary gland

Moran Melamed,[1] Hila Asraf,[1] Noa Livne,[1] Milos Bogdanovic,[1] Anil Shendge,[1] Gilad Shamir,[1] Maayan Mero,[1,3] Omer Adir,[2] Avi Schroeder,[2] Israel Sekler,[1] and Michal Hershfinkel[1,4,*]

[1]Department of Physiology and Cell Biology, School of Bio Medical Research, and the Zelman School of Brain Sciences and Cognition, Faculty of Health Sciences, Ben-Gurion University of the Negev, Beer-Sheva, Israel

[2]The Louis Family Laboratory for Targeted Drug Delivery and Personalized Medicine Technologies, Department of Chemical Engineering, Technion, Haifa, Israel

[3]Present address: Department of Molecular and Human Genetics, Baylor College of Medicine, Houston, TX 77030, USA

[4]Lead contact

*Correspondence: hmichal@bgu.ac.il

https://doi.org/10.1016/j.isci.2025.111912

SUMMARY

Reduced saliva secretion, dry mouth, and loss of taste are debilitating symptoms associated with zinc deficiency. A mechanism for zinc regulation of these processes is lacking. Here, we identified the Zn^{2+} sensing receptor ZnR/GPR39 as a mediator of ion transport in salivary gland epithelium. By monitoring transport of NH_4^+, a surrogate for K^+, we revealed that Zn^{2+} upregulates the Na^+/K^+ ATPase pump activity in parotid and submandibular salivary gland epithelium from wildtype (WT), but not from ZnR/GPR39 knockout (KO), mice. Since Na^+/K^+ ATPase activity is crucial for solute transport, we compared saliva composition in WT and ZnR/GPR39 KO mice and found impaired ionic concentration and reduced saliva secretion in ZnR/GPR39 KO mice. Moreover, mice deficient in ZnR/GPR39 exhibited decreased sensitivity to appetitive Na^+ concentrations. Altogether, we demonstrate that salivary ZnR/GPR39 activity controls saliva ion composition and secretion, and provides a target for therapeutic approaches for dry mouth and taste disorders.

INTRODUCTION

Saliva has an important role of lubricating the oral cavity, facilitating chewing and swallowing, and contributing to enzymatic breakdown of food particles; it is essential for digestion and taste sensation.[1] Dysfunction of salivary glands results in reduced saliva production and xerostomia (dry mouth) that is associated with infection, oral pain, and risk of dental caries.[2] Moreover, changes in the saliva ion composition may interfere with protection of the oral cavity from acidic conditions and impair taste sensation.[3–5] Regulation of saliva ion composition is achieved by balancing ion secretion and absorption in a highly coordinated manner by multiple transporters on the acinar and ductal cells. The salivary acinar cells are responsible for bulk fluid secretion and this requires massive Na^+ and Cl^- efflux. This is largely enabled by the activity of the Na^+/K^+ ATPase pump, which maintains inward Na^+ gradients that power the basolateral NKCC1 providing Cl^- for its apical luminal secretion.[6–9] The ductal cells re-absorb Na^+ and Cl^-, and secrete K^+ and HCO_3^-.[10,11] Re-absorption of Na^+ is mediated by apical ENaC channels, and is then pumped out by the Na^+/K^+ ATPase, which also supports the K^+ efflux, via Ca^{2+}-dependent channels, into the lumen.[10,12–15] It is well established that Ca^{2+} signals maintain the physiological salivary secretion,[8,16] and specifically regulate vectorial ion transport powered by the Na^+/K^+ ATPase. The pump is indeed tightly regulated by the Ca^{2+} rise triggered by muscarinic stimulation[17] or by norepinephrine activation of the α adrenergic receptors.[18]

Zinc, found in the saliva,[19,20] is an essential micronutrient that modulates the physiological activity of epithelial cells.[21,22] Interestingly, dental caries, xerostomia, and taste disorders are also associated with reduced zinc levels.[23–25] Zinc ions (Zn^{2+}) are accumulated in granules in the epithelial cells of the salivary glands.[26,27] Similarly, Zn^{2+} containing vesicles in neurons have an important role in regulating neuronal transmission and the inhibitory tone.[28,29] In the salivary gland, a specific zinc-binding salivary protein gustin was suggested to mediate taste sensation,[30] but the underlying mechanism for Zn^{2+} control of salivation or taste sensing is not well understood.

Signaling by extracellular Zn^{2+} is largely mediated via ZnR/GPR39, a Gq coupled receptor that is activated by physiological concentrations of extracellular Zn^{2+}.[31] Downstream to the release of Ca^{2+} via the IP3 pathway, ZnR/GPR39 activates cellular pathways regulating ion transport by regulating K^+/Cl^- cotransporters.[32,33] In colon epithelial cells, ZnR/GPR39 enhances the basolateral KCC1, thereby controlling Cl^- absorption.[34] Indeed, mice lacking ZnR/GPR39 expression showed enhanced water loss in a dextran sodium sulfate (DSS) model of diarrhea.[34] Upregulation of KCC3 in tamoxifen-resistant breast cancer cells via ZnR/GPR39 enhances cell proliferation, migration, and changes in

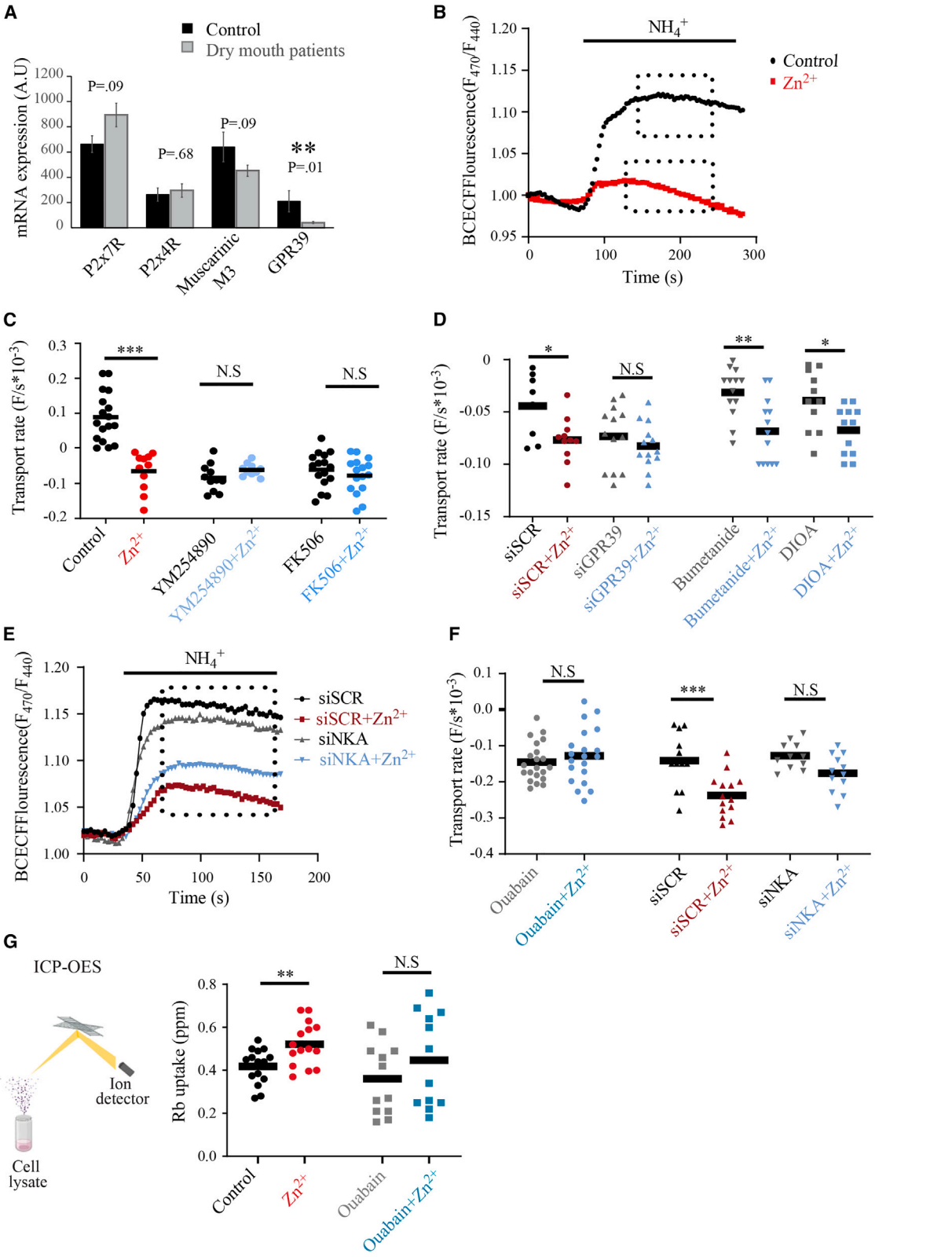

(legend on next page)

cytoskeleton organization.[35] In addition, ZnR/GPR39 dependent activation of the water channel, aquaporin 5, was demonstrated in the HSG salivary cell line.[36]

Importantly, Ca^{2+} signaling such as triggered by ZnR/GPR39 in salivary HSY cells,[37] is suggested to play a major role salivary secretion.[38–40] Here, we show that ZnR/GPR39 modulates solute transport by regulating the Na^+/K^+ ATPase activity in the salivary gland, thus affecting salivary secretion.

RESULTS

We initially studied whether ZnR/GPR39 expression is modulated in human patients with salivary dysfunction by analysis of a gene expression dataset of human parotid tissue (GSE40611, (https://www.ncbi.nlm.nih.gov/geo/)) harvested from patients suffering from xerostomia or healthy individuals.[41,42] This analysis indicated that the level of ZnR/GPR39 mRNA in patients with xerostomia was approximately 4 times lower than in controls (Figure 1A). Importantly, other receptors that are associated with saliva secretion, such as P2X7 and P2X4 purinergic receptors or the muscarinic G-protein coupled receptor M3,[43] did not show such significant difference in expression. This supports a role for ZnR/GPR39 in proper function of the salivary gland.

ZnR/GPR39 activity in HSY salivary cells upregulates Na^+/K^+ ATPase transport

Based on the human data, we asked if ZnR/GPR39 controls ion transport using the HSY salivary ductal cell line that expresses a functional ZnR/GPR39 (Figure S1) and allows easy genetic manipulations.[37] To determine if ZnR/GPR39 regulates K^+ transport, we used NH_4^+ as a surrogate to K^+ while monitoring changes in pH with the fluorescent indicator BCECF.[44,45] Briefly, addition of NH_4Cl (10mM) to the extracellular solution results in diffusion of NH_3 that induces cellular alkalinization, and subsequent transport of NH_4^+ via K^+ transporters induces BCECF acidification.[45] The rates of acidification were increased by Zn^{2+} pre-treatment, 200μM that activates ZnR/GPR39,[46] compared to the rates in control HSY cells (Figures 1B and 1C). Note that the initial alkalinization in the Zn^{2+}-treated cells (red) is also significantly smaller compared to control cells (black), a phenomenon likely due to the robust upregulation of NH_4^+ influx, which induces acidification, concomitant with NH_3 diffusion. To determine if ZnR/GPR39 is responsible for this Zn^{2+} regulation of ion transport, inhibitor for Gαq receptor (YM-254890, 1μM) was used. Following Gαq inhibition, the effect of Zn^{2+} on upregulation of ion transport was reversed (Figure 1C). The ZnR/GPR39 is a Gq-coupled receptor that activates Ca^{2+} signaling (Figure S1), and may trigger calcineurin-dependent activation of the pump. To determine the role of calcineurin in upregulating the K^+ transport activity, an inhibitor of calcineurin, FK506, 100nM, was applied while monitoring NH_4^+ transport. The result in Figure 1C shows that Zn^{2+} upregulation of K^+ transport is abolished by FK506. Finally, to directly study the role of ZnR/GPR39, we used cells transfected with an siGPR39 RNA silencing construct. Quantitative PCR analysis exhibited ~80% silencing of the GPR39 (Figure S1C). We find that silencing of ZnR/GPR39 completely abolished the Zn^{2+}-enhanced NH_4^+ transport activity (Figure 1D). These experiments indicate that Zn^{2+} via ZnR/GPR39 upregulates ion transport in HSY salivary gland cells. Since ZnR/GPR39 regulates KCC transporters in epithelial cells and neurons,[33] we asked if the increased K^+ transport in HSY cells is also mediated by members of this family. Surprisingly, the KCC inhibitor DIOA (100 μM) did not abolish ZnR/GPR39-dependent upregulation of ion transport (Figure 1D). Similarly, application of the NKCC inhibitor, bumetanide (1μM) also failed to abolish Zn^{2+}-dependent upregulation of ion transport (Figure 1D). These results suggest that neither KCC nor NKCC transporters are regulated by ZnR/GPR39 in HSY cells.

Previous studies showed that Na^+/K^+ ATPase activity can also be measured using NH_4^+ as a surrogate to K^+,[47] we therefore applied the same paradigm in the presence of the Na^+/K^+ ATPase pharmacological inhibitor, ouabain (100nM). We find that rates of NH_4^+-dependent acidification in the presence of ouabain were similar in Zn^{2+} treated and control cells (Figure 1F and Figure S2A), suggesting that the Na^+/K^+ ATPase mediates the transport upregulated by Zn^{2+}. Among the isoforms of the

Figure 1. ZnR/GPR39 upregulates Na^+/K^+ ATPase pump activity in HSY cell line

(A) Gene expression of human parotid tissue (GSE40611) from patients suffering from dry mouth or healthy (control) individuals.

(B) HSY cells were loaded with the pH-sensitive fluorescent indicator BCECF (1 μM). Cells were washed with K^+-free Ringer's solution, and addition of NH_4Cl (10 mM) resulted in increase in fluorescence due to NH_3 diffusion. Subsequent NH_4^+ transport, used as surrogate by K^+ transporters, resulted in cytoplasmic acidification. Shown are representative fluorescent signal traces from cells treated with Zn^{2+} (200 μM) or without it. Box marks the regions where initial rates were determined for further analysis.

(C) Rates of acidification during initial 100s of NH_4^+ transport were determined, and column scatterplot of cells treated with or without Zn^{2+} in the presence of YM-254890 (1μM) or FK506 (100nM) are shown.

(D) Column scatterplot of the averaged initial rates of NH_4^+ transport in the presence of siGPR39 and KCC/NKCC inhibitors DIOA (100μM) and bumetanide (1μM).

(E) BCECF fluorescent signal traces of the NH_4^+ paradigm from cells transfected with siNKA α1 or siSCR, which were treated with or without Zn^{2+}.

(F) Column scatterplot of the averaged initial rates of NH_4^+ transport, over initial 100s from maximal signal, suggesting that the Zn^{2+} upregulation of NH_4^+ transport requires ZnR/GPR39 and the Na^+/K^+ ATPase pump.

(G) Rb^+ uptake assay using ICP-OES (left panel) to monitor level on Rb^+ in Zn^{2+} treated HSY cells versus controls. Ouabain-dependent Rb^+ uptake is mediated by the Na^+/K^+ ATPase pump. All column scatterplot values (n = # of slides with ~30 cells per slide, from 3 independent experiments) are presented and the average is marked by the bar, t-test,***$p < 0.001$; **$p < 0.01$; *$p < 0.05$; N.S non-significant. (A) Control ($n = 16$) vs. Dry mouth disease ($n = 30$) patients: P2x7R t(1.754) = 46, $p = 0.086$, P2x4R t(0.413) = 46, $p = 0.682$, M3 t(1.751) = 46, $p = 0.087$, GPR39 t(2.58) = 46, $p = 0.013$. (C) Control ($n = 17$) vs. Zn^{2+} ($n = 11$) t(24.95) = 6.468, p=<0.0001, YM-254890 ($n = 11$) vs. YM-254890+Zn^{2+} ($n = 10$) t(14.36) = 1.735, $p = 0.1041$, FK506 ($n = 16$) vs. FK506 + Zn^{2+} ($n = 16$) t(29.99) = 0.9176, $p = 0.3662$. (D) siSCR ($n = 8$) vs. siSCR+Zn^{2+} ($n = 11$) t(11.84) = 2.520, $p = 0.0271$, siGPR39 ($n = 13$) vs. siGPR39+Zn^{2+} ($n = 13$) t(22.05) = 0.9002, $p = 0.3777$, Bumetanide ($n = 13$) vs. Bumetanide+Zn^{2+} ($n = 13$) t(22.61) = 3.431, $p = 0.0023$, DIOA ($n = 11$) vs. DIOA+Zn^{2+} ($n = 12$) t(19.24) = 2.602, $p = 0.0174$. (F) Ouabain ($n = 21$) vs. Ouabain+Zn^{+2} ($n = 20$) t(34.03) = 0.8402, $p = 0.4067$, siSCR ($n = 14$) vs. siSCR+Zn^{2+} ($n = 14$) t(25.04) = 3.957, $p = 0.0006$, siNKA ($n = 11$) vs. siNKA+Zn^{2+} ($n = 12$) t(19.84) = 2.584, $p = 0.0178$. (G) Control ($n = 15$) vs. Zn^{2+} ($n = 15$) t(26.86) = 3.056, $p = 0.0050$, Ouabain ($n = 12$) vs. Ouabain+Zn^{2+} ($n = 12$) t(20.51) = 1.093, $p = 0.2872$.

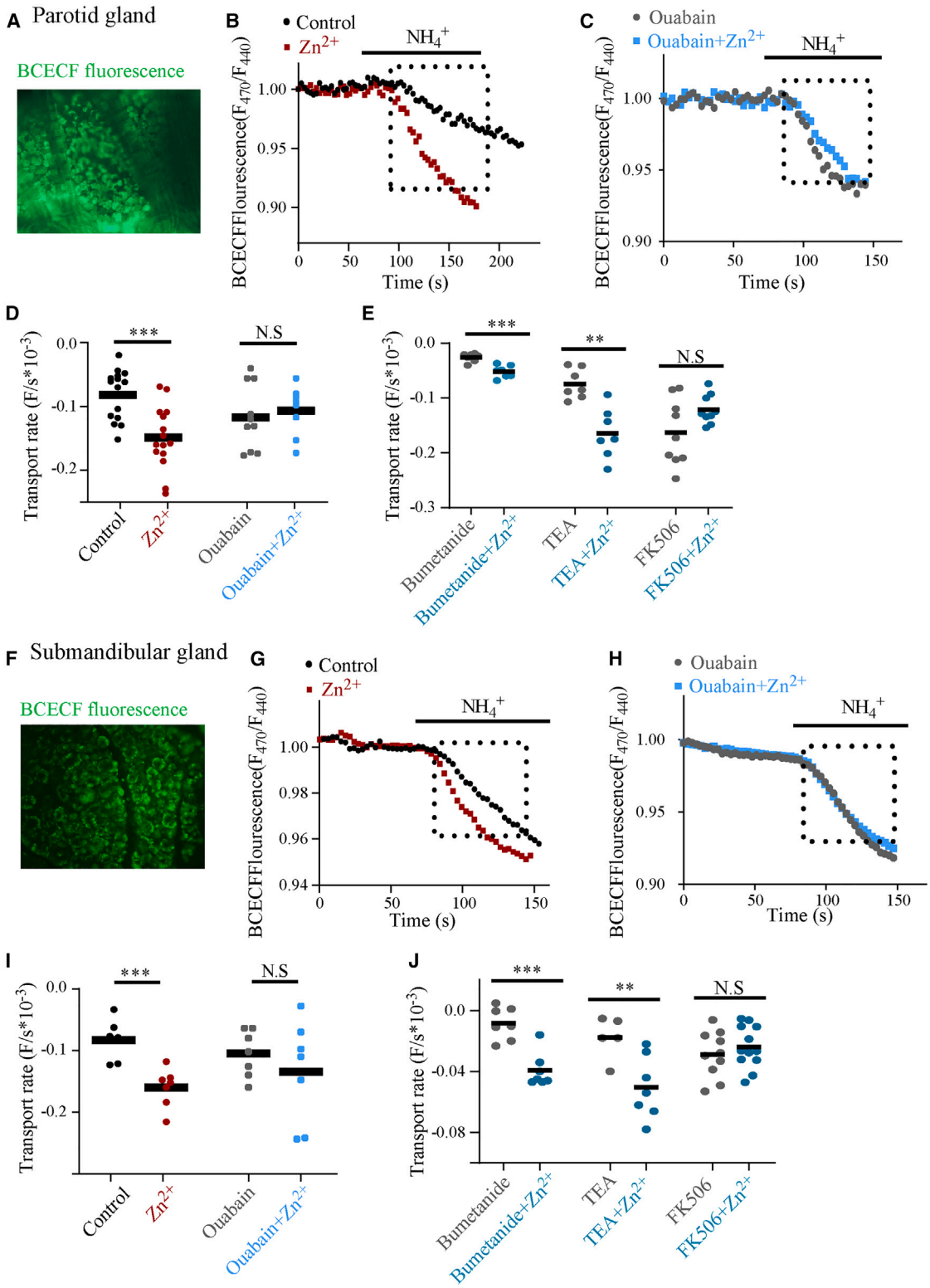

Figure 2. Zn^{2+} upregulates ion transport via the Na^+/K^+ ATPase activity in salivary gland tissues

(A) Representative image of acute slice from mouse parotid gland after loading with the pH-sensitive BCECF dye.

(B) Representative traces of BCECF fluorescence ratio signals from slices that were treated with or without Zn^{2+}. Slices were treated with NH_4Cl at the indicated time, and transport of NH_4^+ acting as a surrogate to K^+ induces cytoplasmic acidification.

(legend continued on next page)

Na^+/K^+ ATPase subunits, the α1 subunit was found in the salivary gland.[12,13] To determine if this subunit mediates the Zn^{2+}-dependent ion transport, cells were transfected with an siRNA construct aimed to silence the α1 subunit of the Na^+/K^+ ATPase pump (siNKA, Figure 1E). Quantitative PCR analysis exhibited more than 50% silencing of the α1 subunit of the Na^+/K^+ ATPase pump in cells transfected with the siRNA construct (Figure S2B). While Zn^{2+}-dependent ion transport activity was observed in cells transfected with the control siRNA (siSCR), Zn^{2+} did not upregulate the activity in cells that do not express α1 Na^+/K^+ ATPase (Figure 1E). Thus, inhibition of Na^+/K^+ ATPase reverses the effect of Zn^{2+}, and ZnR/GPR39, on K^+ transport (Figure 1F). To directly test the regulation of the Na^+/K^+ ATPase by ZnR/GPR39, we exogenously expressed ZnR/GPR39 and the Na^+/K^+ ATPase α1 and β1 subunits in HEK293 cells. Treatment with Zn^{2+} (200μM) increased the rate of NH_4^+ transport only when both the receptor and the pump were expressed, and this increase was reversed by ouabain (Figure S3). These results indicate that ZnR/GPR39 is essential for Zn^{2+}-dependent upregulation of K^+ transport via the Na^+/K^+ ATPase pump. As an additional control, we monitored cellular level of Rb^+ using inductive coupled plasma-optical emission spectroscopy (ICP-OES).[48] While baseline Rb^+ levels were not affected by the Na^+/K^+ ATPase inhibitor ouabain, 200μM Zn^{2+} treatment induced robust Rb^+ transport that was reversed by ouabain (Figure 1G). These results indicate that similar to the fluorescent measurements, ouabain-dependent Rb^+ uptake is increased in Zn^{2+} treated cells. Taken together, these data suggest that Zn^{2+} is required to upregulate the Na^+/K^+ ATPase pump activity in HSY cells.

ZnR/GPR39 activity in salivary glands from WT, but not ZnR/GPR39 KO mice, upregulates K^+ transport that is mediated by the Na^+/K^+ ATPase

To determine a role for ZnR/GPR39 in primary salivary glands, we monitored NH_4^+ transport activity in acute tissue slices from parotid and submandibular (SMG) mouse salivary glands loaded with BCECF (Figures 2A and 2F). Addition of NH_4 (20mM) to the slices was not followed by alkalinization, as found in HSY cells, which can represent very slow diffusion of NH_3 or robust NH_4^+ influx in the primary cells. Nevertheless, salivary gland slices that were pre-treated with 200μM Zn^{2+} showed increased acidification rates compared to controls (Figures 2B and 2G), indicating that NH_4^+ transport is enhanced by Zn^{2+}. However, in slices that were exposed to the Na^+/K^+ ATPase inhibitor, 1mM ouabain, treatment with Zn^{2+} (200μM) did not enhance rates of NH_4^+-dependent acidification (Figures 2C and 2H). This analysis suggests that Zn^{2+} upregulates a ouabain-dependent transporter (Figures 2D and 2I). To determine if the transport activity is directly affected by ZnR/GPR39 or modulated following changes in ion concentrations driven by other transporters, we inhibited major K^+ transport pathways. Salivary slices were treated with the K^+/Cl^- cotransporters (KCC) inhibitor bumetanide, using a concentration of 100μM that inhibits both KCC and Na^+-dependent, NKCC. As shown (Figures 2E and 2J), Zn^{2+} treatment enhanced ion transport in both parotid and SMG in the presence of bumetanide. Similarly, in salivary tissue treated with the non-specific K^+ channels inhibitor tetraethylammonium (TEA, 5mM), Zn^{2+} triggered upregulation of ion transport (Figures 2E and 2J). These results support a conclusion that Zn^{2+} modulates ion transport mediated by the Na^+/K^+ pump. To further study the signaling pathway that is involved in regulation of the pump, we treated the slices with the calcineurin inhibitor, FK506, 200nM, which was associated with regulation of this transporter in the HSY cells. We find that FK506 abolished the effect of Zn^{2+} on transport activity (Figures 2E and 2J). Altogether, these results suggest that Zn^{2+} enhances transport activity mediated by the Na^+/K^+ ATPase, in parotid and SMG salivary tissues.

To determine if ZnR/GPR39, upstream to Zn^{2+} activation of calcineurin, is essential for Zn^{2+}-increased Na^+/K^+ ATPase activity in the salivary glands, we used acute salivary gland tissues from ZnR/GPR39 KO mice.[44,49] Rates of NH_4^+-dependent acidification in ZnR/GPR39 KO parotid or SMG slices that were pre-treated with Zn^{2+} were similar to the rates in control slices, not treated with Zn^{2+} (Figures 3A–3C). These results indicate that ZnR/GPR39 activity is essential for the effect of Zn^{2+} on ion transport via the Na^+/K^+ ATPase pump in salivary gland cells. Impaired expression of Na^+/K^+ ATPase in the ZnR/GPR39 KO tissue could also result in such attenuation of Zn^{2+}-dependent upregulation of ion transport rates. We therefore studied the expression of the α1 subunit of the Na^+/K^+ ATPase in parotid and SMG tissues

(C) Fluorescent signal traces from slices treated with the Na^+/K^+ ATPase inhibitor ouabain (1mM), in the presence of Zn^{2+} or without it, and exposed to the NH_4^+ paradigm as in B. Box marks the regions where initial rates were determined for further analysis.
(D) Rates of acidification during initial 50s of NH_4^+ transport (see B-C) were determined, and are presented in the column scatterplot, representing NH_4^+ transport. Ouabain-sensitive transport is mediated by the Na^+/K^+ ATPase pump.
(E) Column scatterplot of the averaged initial rates of NH_4^+ transport in the presence of K^+ transporters inhibitors: bumetanide (100μM) or TEA (5mM) or the calcineurin inhibitor, FK506 (200nM).
(F) Representative image of BCECF loaded submandibular acute slice.
(G) Representative trace of BCECF fluorescent ratio signals of the NH_4^+ paradigm from slices that were treated with or without Zn^{2+} as in B.
(H) Fluorescent BCECF signal traces of the NH_4^+ paradigm from slices treated with ouabain (1mM) or without it. Box marks the regions where initial rates were determined for further analysis.
(I) Rates of acidification during initial 50s of NH_4^+ transport (see B-C) were determined, and are presented in the column scatterplot, representing NH_4^+ transport. Ouabain-sensitive transport is mediated by the Na^+/K^+ ATPase pump.
(J) Rates of BCECF signal changes during initial acidification of the NH_4^+ paradigm from slices treated with the KCC inhibitor, bumetanide (100 μM), of the K^+ channels inhibitor, TEA (5mM) or FK506 (200nM). All column scatterplot values (n = # of slices with ~30 cells per slide, from 3 independent mice) are presented and the average is marked by the bar, t-test,***$p < 0.001$; N.S non-significant. (D) Control ($n = 15$) vs. Zn^{2+} ($n = 15$) t(26.36) = 4.168, $p = 0.0003$, Ouabain ($n = 10$) vs. Ouabain+Zn^{2+} ($n = 8$) t(15.98) = 0.4699, $p = 0.6448$. (E) Bumetanide ($n = 7$) vs. Bumetanide+Zn^{2+} ($n = 7$) t(10.51) = 5.074, $p = 0.0004$, TEA($n = 7$) vs. TEA+Zn^{2+} ($n = 7$) t(9.794) = 4.475, $p = 0.0013$, FK506 ($n = 9$) vs. FK506+Zn^{2+} ($n = 9$) t(11.02) = 1.899, $p = 0.0840$. (I) Control ($n = 7$) vs. Zn^{2+} ($n = 7$) t(12) = 4.581, $p = 0.0006$, Ouabain ($n = 7$) vs. Ouabain+Zn^{2+} ($n = 7$) t(8.424) = 0.8459, $p = 0.4210$. (J) Bumetanide ($n = 7$) vs. Bumetanide+Zn^{2+} ($n = 7$) t(11.96) = 5.236, $p = 0.0002$, TEA ($n = 5$) vs. TEA+Zn^{2+} ($n = 7$) t(9.994) = 3.295, $p = 0.0081$, FK506 ($n = 10$) vs. FK506+Zn^{2+} ($n = 12$) t(18.49) = 0.7986, $p = 0.4346$.

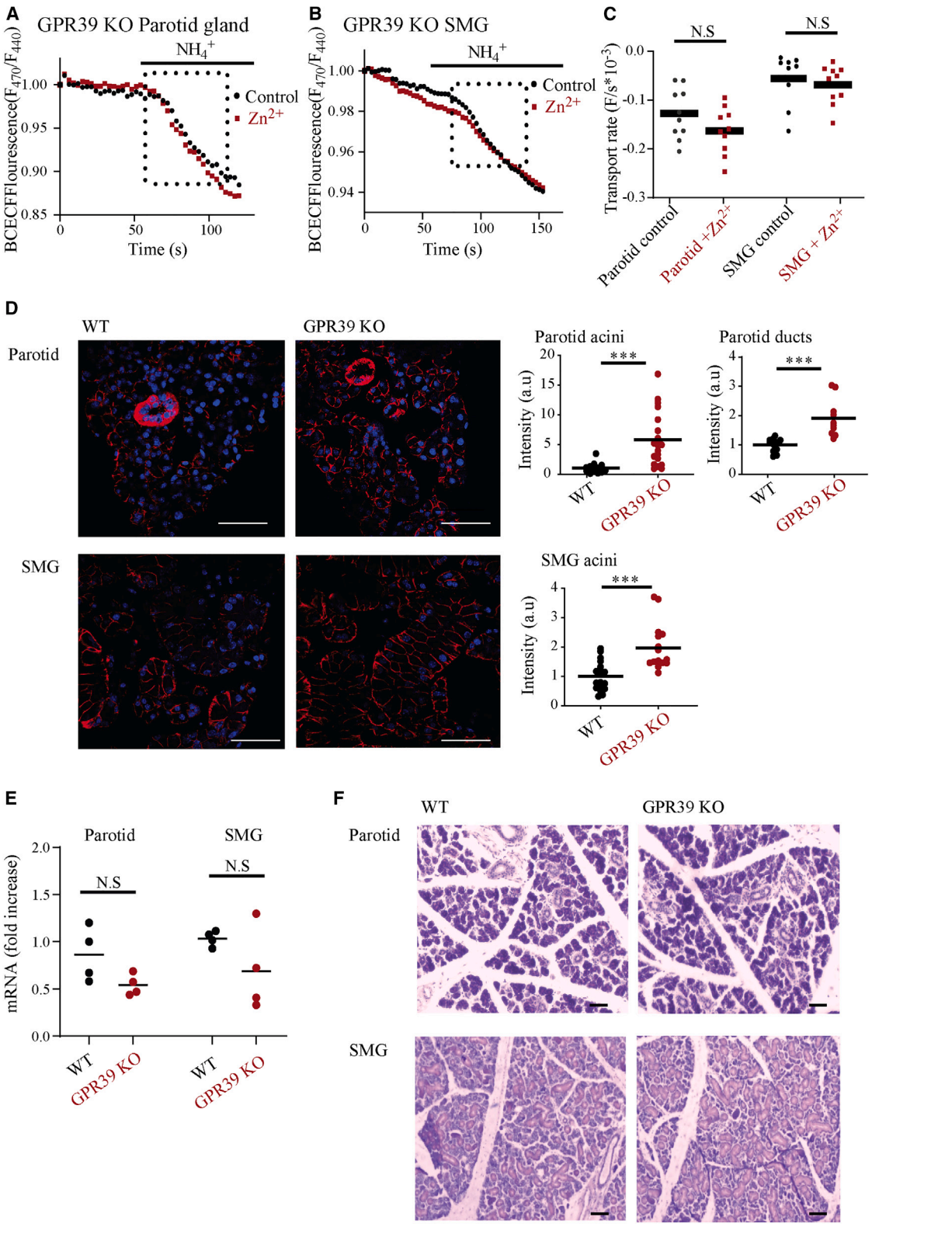

(legend on next page)

(Figure 3D). Surprisingly, we observed a dramatic increase in Na^+/K^+ ATPase protein expression, that was apparent on the basolateral region of cells in ducts and acini, in immunostained tissues from ZnR/GPR39 KO compared to WT glands. This increase was about 4-fold in acini in the parotid gland, and 2-fold in SMG acini (Figure 3D). In addition, ducts that were particularly prominent in slices from parotid tissue also showed about 2-fold increase in Na^+/K^+ ATPase expression in the ZnR/GPR39 KO tissues. Analysis of mRNA expression level showed that no significant changes at the transcription level of the Na^+/K^+ ATPase in parotid and SMG tissues from ZnR/GPR39 KO mice compared to WT mice (Figure 3E). Moreover, note that no differences in general morphology were observed between WT or ZnR/GPR39 KO tissues from parotid and SMG stained with H&E, when comparing the size of ducts or acini (Figure 3F). Altogether our results indicate that direct regulation of Zn^{2+} via ZnR/GPR39 on Na^+/K^+ ATPase activity controls ion transport.

Deletion of ZnR/GPR39 modulates saliva secretion and composition and reduces salt taste sensitivity

Since regulation of the Na^+/K^+ ATPase affects Na^+, K^+ and Cl^-, transport by the salivary epithelial cells, we predicted that ZnR/GPR39 regulation of this pump will modulate saliva ion concentrations. We therefore compared ion concentrations in saliva samples obtained from ZnR/GPR39 KO versus WT mice. We found that both, Na^+ and K^+, concentrations were elevated in saliva from ZnR/GPR39 KO mice, but there was no significant change in Cl^- concentration (Figure 4A). This suggested that in the absence of ZnR/GPR39, saliva composition is abrogated. To determine if the effect in ZnR/GPR39 KO mice may be modulated by different levels of salivary Zn^{2+}, we measured Zn^{2+} concentration in saliva samples obtained from ZnR/GPR39 KO or WT mice using ICP-OES. We find that in both genotypes the concentration is about 0.9 μM (corresponding to about 56 ppb) with no difference between WT versus ZnR/GPR39 KO mice (Figure 4B). Note that this concentration in the saliva is likely affected by protein binding Zn^{2+} and may be lower compared to transient local concentration in the lumen of the gland. To determine if ZnR/GPR39 affects salivary secretion, we measured the amount of secreted saliva. We monitored the weight of saliva accumulation following treatment with pilocarpine (10 mg/kg). We found that the secreted saliva in ZnR/GPR39 KO mice was lower compared to WT mice (Figure 4C).

Salivary secretion is essential for taste sensation,[50] hence the unbalanced ion and water composition of saliva in ZnR/GPR39 deficient mice may affect their taste sensation. To test the effect of ZnR/GPR39 on taste sensation we used the two bottle preference test, in which the mice can choose to drink from a bottle containing water or a bottle containing a tastant (Figure 4D). We compared two concentrations of NaCl, 100mM that is attractive and 500mM that is aversive to mice.[51] We find that at 100mM NaCl, the WT mice preferred the salty water and drank from this bottle more than 50% random choice. However, ZnR/GPR39 KO mice could not distinguish between the tastant and control bottles, and drank randomly (50%) from each of them (Figure 4D). In contrast, both WT and ZnR/GPR39 KO mice sensed the aversive 500mM concentration of NaCl, and drank much less than 50% of this bottle compared to the water bottle. As control, we used high saccharine (0.5%) concentration that is also attractive, but is expected to activate pathways that are less sensitive to Na^+ or K^+ concentrations in the saliva.[52,53] Indeed, at this very sweet concentration, both WT and ZnR/GPR39 KO mice preferred the bottle containing saccharine, to a similar level. These results suggest that lack of ZnR/GPR39, which results in unbalanced saliva composition, can lead to taste sensation disorders.

DISCUSSION

Nutritional studies associated zinc with modulation of salivary secretion and taste sensation in humans[54] and animal studies.[55] The results presented here show a functional ZnR/GPR39 in salivary gland epithelial cells, which modulates saliva ion composition and secretion. Activity of ZnR/GPR39 was previously linked to Zn^{2+}-dependent regulation of epithelial ion transport, which was mediated via modulation of distinct family members of the K^+/Cl^- (KCC) cotransporters in intestinal epithelium and breast cancer cells.[33] Surprisingly, in the salivary epithelium ZnR/GPR39 did not regulate the KCC transporters, but the Na^+/K^+ ATPase pump. Indirect regulation of this transporter due to changes of ion concentration has been widely described, particularly changes in K^+ levels.[56,57] Thus, ZnR/GPR39 modulation of K^+ transport by Zn^{2+}, such as previously monitored by regulation of KCC1-3,[32,34,35,44] may indirectly affect the Na^+/K^+ ATPase pump activity. In addition, activity of the basolateral Na^+-dependent KCC (NKCC1) transporter plays a role in ion transport in

Figure 3. ZnR/GPR39 is essential for Zn^{2+}-dependent upregulation of Na^+/K^+ ATPase pump activity in salivary gland tissue

(A) BCECF fluorescent signal traces from ZnR/GPR39 KO parotid tissue slices that were treated with or without Zn^{2+}, and exposed to the NH_4^+ paradigm.

(B) BCECF fluorescent signal traces of slices from ZnR/GPR39 KO submandibular tissue that were treated with or without Zn^{2+}, and exposed to the NH_4^+ paradigm. Box marks the region where the initial rate was determined for further analysis.

(C) Rates of acidification during initial 50s of NH_4^+ transport (see A-B) were determined, and presented in the column scatterplot.

(D) Left panel, representative confocal images (60X) of Na^+/K^+ ATPase immunolabeling (red) and DAPI nuclei-staining (blue) from parotid and submandibular glands from WT and ZnR/GPR39 KO mice. Right panel, quantification of Na^+/K^+ ATPase expression in acini and ducts in parotid tissue or acini only in submandibular tissue, where ducts were not clearly stained.

(E) Na^+/K^+ ATPase mRNA expression levels were determined using qPCR from parotid and submandibular tissues. Values were normalized to the housekeeping gene β-actin.

(F) Histological H&E staining of parotid and submandibular tissues from WT or ZnR/GPR39 KO mice. Scale bar on microscope images is 50μm. All column scatterplot values (n = # of slices/sections, from 3 independent mice) are presented and the average is marked by the bar, t-test, $^{***}p < 0.001$; N.S non-significant. (C) Parotid control ($n = 10$) vs. Parotid+Zn^{2+} ($n = 10$) t(17.87) = 1.598, $p = 0.1276$, SMG Control ($n = 9$) vs. SMG+Zn^{2+} ($n = 10$) t(14.71) = 0.5737, $p = 0.5749$. (D) Parotid acini- WT ($n = 16$) vs. GPR39 KO ($n = 20$) t(20.50) = 4.654, $p = 0.0001$, Parotid ducts- WT ($n = 13$) vs. GPR39 KO ($n = 10$) t(10.60) = 4.282, $p = 0.0014$, SMG acini- WT ($n = 17$) vs. GPR39 KO ($n = 17$) t(25.65) = 4.161, $p = 0.0003$. (E) Parotid WT ($n = 4$) vs. GPR39 KO ($n = 4$) t(3.899) = 2.072 $p = 0.1088$, SMG WT ($n = 4$) vs. GPR39 KO ($n = 4$) t(1.543) = 3.199, $p = 0.2150$.

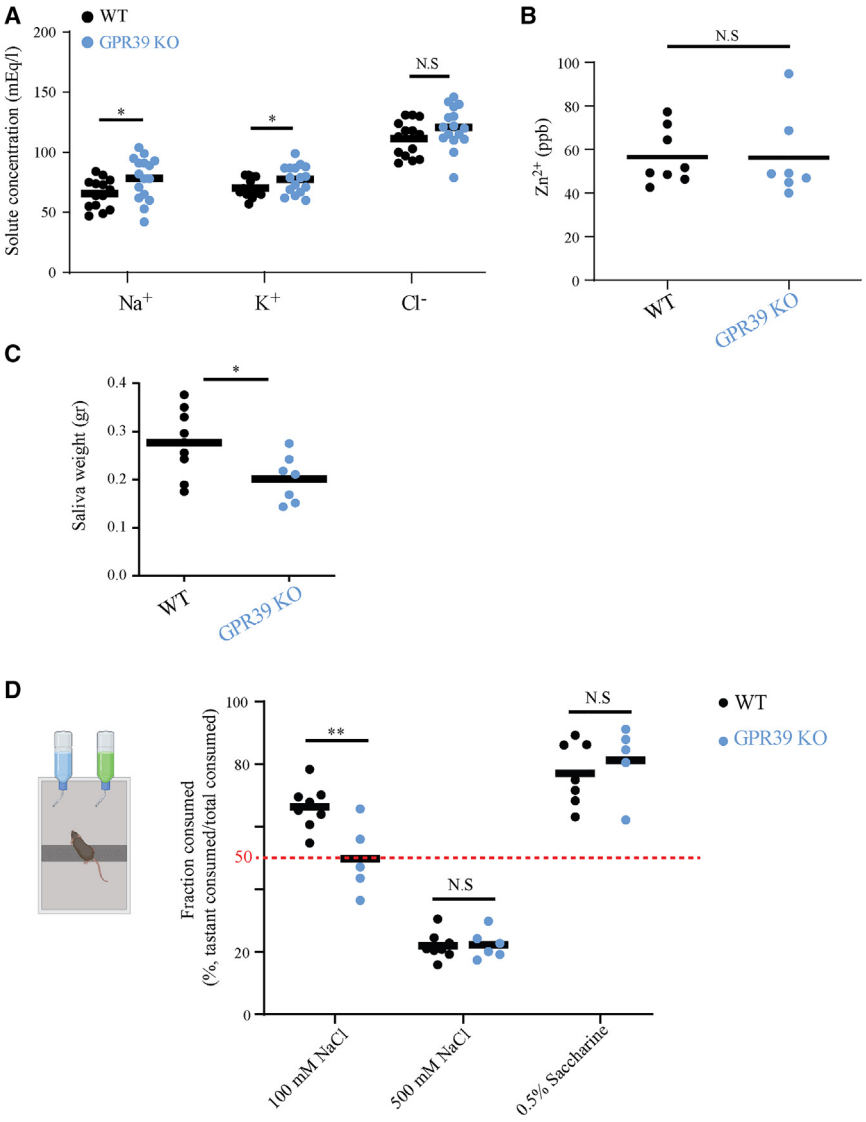

Figure 4. Impaired saliva secretion and composition and abrogated taste sensation in ZnR/GPR39 KO mice

(A) Normalized level of ion content of K^+, Na^+ and Cl^- in saliva of WT and ZnR/GPR39 KO mice.

(B) Normalized level of Zn^{2+} in saliva from WT or ZnR/GPR39 KO mice.

(C) The mass of saliva secretion, collected during a 15 min period, from ZnR/GPR39 KO and WT mice.

(D) Two bottle preference test, fraction of tastant intake normalized to total intake. The red line indicates a preference score of 50%, showing no preference toward either of the tastants. Column scatterplot values are presented and the average is marked by the bar, t-test, $^{**}p < 0.01$; $^{*}p < 0.05$; N.S non-significant. (A) WT ($n = 14$) vs. GPR39 KO ($n = 16$): Na^+ t(26.54) = 2.270, $p = 0.0315$, K^+ t(26.63) = 2.076, $p = 0.0477$, Cl^- t(28.00) = 1.599, $p = 0.1210$. (B) WT ($n = 8$) vs. GPR39 KO ($n = 7$) t(10.28) = 0.03569, $p = 0.9722$. (C) WT ($n = 8$) vs. GPR39 KO ($n = 7$) t(13.93) = 2.564, $p = 0.0226$. (D) WT ($n = 8$) vs. GPR39 KO ($n = 5$): 100mM NaCl t(11) = 3.286, $p = 0.0073$, 500mM NaCl WT ($n = 8$) vs. GPR39 KO ($n = 6$): t(10.70) = 0.1451, $p = 0.8873$, 0.5% Saccharine WT ($n = 7$) vs. GPR39 KO ($n = 5$): t(8.093) = 0.6512, $p = 0.5329$.

salivary cells.[58,59] However, inhibition of KCC or NKCC in the HSY cells did not reverse the effect of Zn^{2+} on ion transport. Further, in the salivary gland tissues our results show that neither inhibition of KCC/NKCC, using bumetanide at concentrations that inhibit both transporters, nor the non-specific K^+ channel blocker TEA, reversed Zn^{2+}-dependent regulation of transport. In contrast, silencing of the pump in HSY cells or addition of the Na^+/K^+ ATPase pump inhibitor ouabain to parotid or SMG tissue completely reversed the Zn^{2+}-dependent upregulation of ion transport. In addition, while Zn^{2+}-dependent upregulation of transport activity was clearly seen in WT salivary tissue sections, we did not see this upregulation in the ZnR/GPR39 KO salivary tissues. Thus, our data support the conclusion that Zn^{2+}-dependent activation of ZnR/GPR39 upregulates the Na^+/K^+ ATPase.

To identify the transporter that is regulated by ZnR/GPR39 in HSY cells and salivary glands tissue, we used the pharmacological inhibitor ouabain, due to its relative selectivity to the Na^+/K^+ ATPase.[60,61] While in both, cell line and salivary glands tissue, ouabain abolished the ZnR/GPR39 upregulation of K^+ transport, we found differences in the concentration of ouabain required to abolish the activity of the of Na^+/K^+ ATPase in the salivary mouse tissues (1mM) compared to the human cell line (100nM). This is likely due to well established differences in affinity of ouabain in specific species.[62,63] The inhibitory effect of ouabain strongly supports the role of ZnR/GPR39 in modulating Na^+/K^+ ATPase-dependent K^+ transport in WT but not in ZnR/GPR39 KO salivary epithelium. Using confocal microscopy, we found that the Na^+/K^+ ATPase α1 subunit[64] is expressed on salivary parotid and submandibular gland acinar and duct cells, with higher levels in the duct cells. Since the measured transport activity may be affected by the expression of the protein, we compared the level of expression of the Na^+/K^+ ATPase α1 subunit between WT and ZnR/GPR39 KO tissues. We found that mRNA levels are similar between the genotypes, but the protein expression of the Na^+/K^+ ATPase α1 subunit was more abundant in ZnR/GPR39 KO mice compared to WT. Post-transcriptional regulation of the pump expression or degradation is well documented,[65–67] and a similar effect of stable mRNA versus modified protein was also found in lung or intestinal epithelial cells.[68,69] Since the ZnR/GPR39 KO mouse model is a global knockout, developmental compensation may enhance the expression of the Na^+/K^+ ATPase that is however not functionally upregulated by Zn^{2+} in this model. Note that we did not detect upregulation of the baseline transport rates

between the WT and ZnR/GPR39 KO tissues, suggesting that increased expression does not result in increased function of the pump under baseline conditions. We cannot rule out, however, compensatory regulation in the salivary glands of ZnR/GPR39 KO mice that is activated via a different pathway, such as purinergic or β-adrenergic receptors.[70] Moreover, the effect of ZnR/GPR39 modulation of the transport activity is monitored in acute tissue slices, where we could not discriminate between ducts and acini, which may show different expression level of the Na^+/K^+ ATPase. Importantly, the effect of Zn^{2+} was monitored in multiple regions of interest, suggesting it is mediated in the acini cells that are abundant in the preparation and likely also in the ducts. It would be of interest to further assess the role of ZnR/GPR39 in a conditional knockout model of the receptor that is specific to various cells of the salivary glands and will reduce compensatory developmental effects.

Several G-protein coupled receptor ligands, such as dopamine, adrenaline and parathyroid hormone, regulate the Na^+/K^+ ATPase pump activity.[71,72] This modulation of the activity of the Na^+/K^+ ATPase is essential for electrolyte homeostasis and is highly regulated by protein kinase A and C.[63,73] Specific activation of PKC isoforms by G-protein coupled receptors, via Ca^{2+} signaling, in addition to activation of the MAPK signaling, may stimulate or attenuate Na^+/K^+ ATPase activity.[74,75] The Gq-dependent Ca^{2+}-MAPK pathway is triggered by ZnR/GPR39 and can therefore mediate the effects of ZnR/GPR39 on ion transport in the salivary glands,[31,33,37] Specifically, activation of Gq signaling and calcineurin was previously shown to mediate the regulation of Na^+/K^+ ATPase activity by the α1-adrenergic receptor.[71] Inhibition of calcineurin in astrocytes also inhibited the Na^+/K^+ ATPase activity, which modulated neuronal excitability.[76] In HSY cells and in salivary parotid or SMG tissues, we also show that inhibition of calcineurin, with FK506, reverses the Zn^{2+}-dependent upregulation of transport. The importance of G-protein coupled receptor regulation of Na^+/K^+ ATPase activity is demonstrated by the effect of a mutation of the G-protein coupled GPR35, which fails to interact with the pump in macrophages and intestinal epithelial cells, and is associated with inflammatory diseases and a higher cancer risk.[48] Previous studies show ZnR/GPR39 has a role in epithelial breast cancer,[35] via regulation of KCC, It would be interesting to determine a role for ZnR/GPR39 regulation of the Na^+/K^+ ATPase in carcinogenesis in the salivary gland.

We show that ZnR/GPR39 is an upstream regulator of Na^+/K^+ ATPase activity in salivary gland tissues, where this transporter maintains the Na^+ and K^+ gradients, thus providing the driving force for other transporters and modulating saliva secretion.[10,77,78] Extracellular concentrations of free-Zn^{2+} are low under baseline conditions, due to its rapid chelation by numerous proteins, yet transient release of this ion facilitates high local concentrations of Zn^{2+}.[79–81] Our previous studies show that Zn^{2+} activates ZnR/GPR39, and its release from epithelial cells or neurons can modulate the activity of the receptor, while chelation of this ion reverses this activation.[31,34,44,46,79,82] Accumulation of Zn^{2+} in cytoplasmic vesicles in the salivary gland epithelium, similar to what was shown in neurons, was described almost three decades ago,[26] yet its physiological targets were not known. As such, activity of the ZnR/GPR39 in the salivary gland may be triggered by luminal Zn^{2+} transients following release of secretory granules. Another possible regulator of ZnR/GPR39 is release of Zn^{2+} from nerve fibers on the basolateral side of the epithelial cells.[28,63] Interestingly, glutamate that is co-released with Zn^{2+}, was previously linked to upregulation of the Na^+/K^+ ATPase activity by increased membrane expression of the transporter,[83] a pathway that should be further studied in the context of ZnR/GPR39.

Saliva plays a vital role in taste and flavor perception by directly affecting the dissolution of food in the mouth, and also by bathing the taste receptors in the mouth with the dissolved flavor molecules.[72,84,85] Taste sensation has an important role of assessing the nutritional value of food and preventing the consumption of harmful substances. Changes in the salivary ion composition can directly affect ion channels, such as the ENaC or modulate salty or sour taste sensation.[85,86] We find that saliva ion concentration is unbalanced in global ZnR/GPR39 KO mice, with higher concentrations of Na^+ (∼20%) and K^+ (∼10%), compared to saliva from WT mice. These results may be masked by developmental compensatory mechanisms, which can be minimized using a conditional KO model. Yet, previous animal models showed similar effects of ouabain treatment, which inhibits the Na^+/K^+ ATPase activity. In rats, ouabain reduced saliva secretion and elevated saliva K^+ concentrations in a dose-dependent manner.[87,88] Treatment of dogs with ouabain also resulted in abrogated Na^+ and K^+ concentrations in the saliva.[89] Finally, in hypertensive patients, treatment with ouabain, and the NKCC inhibitor furosemide, also resulted in impaired salivary electrolyte concentrations.[90] Thus, changes in electrolyte concentration and saliva secretion found in ZnR/GPR39 KO mice, in which Na^+/K^+ ATPase activity is not upregulated by Zn^{2+}, are in accordance with changes induced by inhibition of the pump using ouabain.

The changes in salivary ion concentration suggested that ZnR/GPR39 may affect taste sensation,[50] which we tested using an established two-bottle assay.[86] We focused on salty taste, which in low concentration is appetitive and in high concentration it becomes powerfully aversive.[51] The ZnR/GPR39 KO mice showed that they could identify the aversive concentration of salt, but could not distinguish between water and low appetitive salt concentration. This suggested that indeed ZnR/GPR39 deficiency impairs saliva secretion and thereby taste. Since perception of taste is also regulated by the taste buds, using a global ZnR/GPR39 KO mouse we cannot exclude that this change on taste acuity may result from the activity of taste buds on the tongue in ZnR/GPR39 KO mice. The activity of the taste buds, and sensation of taste are closely associated with food intake,[91,92] yet a previous study demonstrated there was no change in food intake in the ZnR/GPR39 global KO compared to WT mice.[84] While this may suggest that ZnR/GPR39 KO mice maintain proper taste bud function, these results may also be explained by interaction of the chow with saliva that can modify its ion concentration, thereby reducing the effect of salivary imbalance. Moreover, taste sensation is deciphered in the brain,[93,94] and we have previously shown that ZnR/GPR39 regulates neuronal excitability.[44,82,95] Thus, the effect of ZnR/GPR39 KO on taste preferences found here may also be modulated by neuronal dysfunction. Use of a conditional

salivary specific KO of the ZnR/GPR39 will be required to specifically dissect the behavioral implication of the abrogated saliva composition in the global ZnR/GPR39 KO mouse. Nevertheless, our results suggest that ZnR/GPR39 activity is essential for saliva ion composition and rate of secretion in addition to modulating taste sensation. A hallmark of zinc deficiency is indeed loss of taste and dysfunction of salivary secretion.[23,96,97] Low zinc levels are common in the elderly population[98,99] and in anorexia nervosa patients.[100] Our results suggest that loss of zinc may also affect salivation and underlie the impaired oral health seen in the elderly or anorexia patients. While fibrosis of glandular tissue was observed in the elderly population and associated with impaired saliva secretion, we found that loss of ZnR/GPR39, in the ZnR/GPR39 KO mice, did not induce morphological changes in the parenchyma, acini, or ducts size or numbers, compared to WT mice. Finally, numerous studies suggested that zinc supplementation is effective in treatment of idiopathic taste disorders.[64,101,102] While zinc supplementation may affect multiple zinc-dependent processes, our findings that ZnR/GPR39 activation enhances saliva secretion and maintains its composition provide an important handle for selectively regulating saliva secretion and oral health.

The results presented here elucidate a mechanism that may underlie the effect of zinc deficiency on saliva regulation, mediated by ZnR/GPR39 regulation of ion transport via the Na^+/K^+ ATPase in salivary glands. Based on the well-established role of salivary ion concentration on taste sensation, we further link ZnR/GPR39 activity to salt taste sensitivity. Regulation of ZnR/GPR39 activity on saliva production may therefore serve as an upstream target for ameliorating symptoms of dry mouth.

Limitations of the study

We show a role for ZnR/GPR39 in regulating salivary function and affecting taste acuity using the ZnR/GPR39 KO mouse model. The regulation of Na^+/K^+ ATPase by the ZnR/GPR39 is shown in a model cell line and in the mouse tissue, however, the precise molecular mechanisms of this interaction are not fully elucidated. In addition, use of human tissue, while monitoring the expression of ZnR/GPR39, will be required to determine how the receptor regulates saliva secretion and dry mouth disease in humans.

RESOURCE AVAILABILITY

Lead contact

Further information and requests for resources and reagents should be directed to and will be fulfilled by the lead contact, Michal Hershfinkel (hmichal@bgu.ac.il).

Materials availability

This study did not generate new unique reagents.

Data and code availability

All data needed to evaluate the conclusions in the paper are present in the paper. Additional data related to this paper may be requested and will be shared upon request from the lead contact.

ACKNOWLEDGMENTS

This work was supported by the Israel Science Foundation (ISF Grant 812/20) to M.H.

AUTHOR CONTRIBUTIONS

M. Melamed, H.A., and M.H. designed experiments. M. Melamed, H.A., N.L., M.B., G.S., M. Mero, O.A., and A.S. conducted experiments and performed data analysis. M. Melamed, I.S., and M.H. wrote the manuscript.

DECLARATION OF INTERESTS

The authors declare that they have no competing interests.

STAR★METHODS

Detailed methods are provided in the online version of this paper and include the following:

- KEY RESOURCES TABLE
- EXPERIMENTAL MODEL AND STUDY PARTICIPANT DETAILS
- METHOD DETAILS
  - Rb^+ uptake assay
  - Fluorescent imaging
  - NH_4Cl paradigm for monitoring K^+ transport
  - Animals
  - Tissue preparation for live fluorescence imaging
  - Immunofluorescent histological analysis of salivary gland tissue sections
  - Salivary secretion measurements
  - Taste acuity measurements
- QUANTIFICATION AND STATISTICAL ANALYSIS

SUPPLEMENTAL INFORMATION

Supplemental information can be found online at https://doi.org/10.1016/j.isci.2025.111912.

Received: May 20, 2024
Revised: October 28, 2024
Accepted: January 24, 2025
Published: January 28, 2025

REFERENCES

1. Carpenter, G.H. (2013). The secretion, components, and properties of saliva. Annu. Rev. Food Sci. Technol. *4*, 267–276.
2. Roussa, E. (2011). Channels and transporters in salivary glands. Cell Tissue Res. *343*, 263–287.
3. Matsuo, R. (2000). Role of saliva in the maintenance of taste sensitivity. Crit. Rev. Oral Biol. Med. *11*, 216–229.
4. Delwiche, J., and O'Mahony, M. (1996). Changes in secreted salivary sodium are sufficient to alter salt taste sensitivity: use of signal detection measures with continuous monitoring of the oral environment. Physiol. Behav. *59*, 605–611.
5. Matsuo, R., and Yamamoto, T. (1992). Effects of inorganic constituents of saliva on taste responses of the rat chorda tympani nerve. Brain Res. *583*, 71–80.
6. Romanenko, V.G., Nakamoto, T., Srivastava, A., Begenisich, T., and Melvin, J.E. (2007). Regulation of membrane potential and fluid secretion by Ca2+-activated K+ channels in mouse submandibular glands. J. Physiol. *581*, 801–817.
7. Melvin, J.E., Yule, D., Shuttleworth, T., and Begenisich, T. (2005). Regulation of fluid and electrolyte secretion in salivary gland acinar cells. Annu. Rev. Physiol. *67*, 445–469.
8. Sneyd, J., Vera-Sigüenza, E., Rugis, J., Pages, N., and Yule, D.I. (2021). Calcium Dynamics and Water Transport in Salivary Acinar Cells. Bull. Math. Biol. *83*, 31.

9. Lee, M.G., Ohana, E., Park, H.W., Yang, D., and Muallem, S. (2012). Molecular mechanism of pancreatic and salivary gland fluid and HCO3 secretion. Physiol. Rev. *92*, 39–74.
10. Ohana, E. (2015). Transepithelial ion transport across duct cells of the salivary gland. Oral Dis. *21*, 826–835.
11. Catalán, M.A., Nakamoto, T., and Melvin, J.E. (2009). The salivary gland fluid secretion mechanism. J. Med. Invest. *56*, 192–196.
12. Winston, D.C., Hennigar, R.A., Spicer, S.S., Garrett, J.R., and Schulte, B.A. (1988). Immunohistochemical localization of Na+,K+-ATPase in rodent and human salivary and lacrimal glands. J. Histochem. Cytochem. *36*, 1139–1145.
13. Soltoff, S.P., Asara, J.M., and Hedden, L. (2010). Regulation and identification of Na,K-ATPase alpha1 subunit phosphorylation in rat parotid acinar cells. J. Biol. Chem. *285*, 36330–36338.
14. Turner, R.J. (1993). Mechanisms of fluid secretion by salivary glands. Ann. N. Y. Acad. Sci. *694*, 24–35.
15. Su, S., Rugis, J., Wahl, A., Doak, S., Li, Y., Suresh, V., Yule, D., and Sneyd, J. (2022). A Mathematical Model of Salivary Gland Duct Cells. Bull. Math. Biol. *84*, 84.
16. Takano, T., Wahl, A.M., Huang, K.T., Narita, T., Rugis, J., Sneyd, J., and Yule, D.I. (2021). Highly localized intracellular Ca(2+) signals promote optimal salivary gland fluid secretion. Elife *10*, 66170.
17. Passafaro, D., Reina, S., Sterin-Borda, L., and Borda, E. (2010). Cholinergic autoantibodies from primary Sjögren's syndrome modulate submandibular gland Na+/K+-ATPase activity via prostaglandin E2 and cyclic AMP. Eur. J. Oral Sci. *118*, 131–138.
18. Insel, P.A., and Snavely, M.D. (1981). Catecholamines and the kidney: receptors and renal function. Annu. Rev. Physiol. *43*, 625–636.
19. Bales, C.W., Freeland-Graves, J.H., Askey, S., Behmardi, F., Pobocik, R.S., Fickel, J.J., and Greenlee, P. (1990). Zinc, magnesium, copper, and protein concentrations in human saliva: age- and sex-related differences. Am. J. Clin. Nutr. *51*, 462–469.
20. Solomons, N.W. (1979). On the assessment of zinc and copper nutriture in man. Am. J. Clin. Nutr. *32*, 856–871.
21. Hara, T., Takeda, T.A., Takagishi, T., Fukue, K., Kambe, T., and Fukada, T. (2017). Physiological roles of zinc transporters: molecular and genetic importance in zinc homeostasis. J. Physiol. Sci. *67*, 283–301.
22. Levaot, N., and Hershfinkel, M. (2018). How cellular Zn(2+) signaling drives physiological functions. Cell Calcium *75*, 53–63.
23. Tanaka, M. (2002). Secretory function of the salivary gland in patients with taste disorders or xerostomia: correlation with zinc deficiency. Acta Otolaryngol. Suppl. *546*, 134–141.
24. Tsuchiya, H. (2023). Treatments of COVID-19-Associated Taste and Saliva Secretory Disorders. Dent. J. *11*, 140.
25. Alqahtani, A.A., Alhalabi, F., and Alam, M.K. (2024). Salivary elemental signature of dental caries: a systematic review and meta-analysis of ionomics studies. Odontology *112*, 27–50.
26. Frederickson, C.J., Pérez-Clausell, J., and Danscher, G. (1987). Zinc-containing 7S-NGF complex. Evidence from zinc histochemistry for localization in salivary secretory granules. J. Histochem. Cytochem. *35*, 579–583.
27. Ishii, K., Sato, M., Akita, M., and Tomita, H. (1999). Localization of zinc in the rat submandibular gland and the effect of its deficiency on salivary secretion. Ann. Otol. Rhinol. Laryngol. *108*, 300–308.
28. Krall, R.F., Tzounopoulos, T., and Aizenman, E. (2021). The Function and Regulation of Zinc in the Brain. Neuroscience *457*, 235–258.
29. McAllister, B.B., and Dyck, R.H. (2017). Zinc transporter 3 (ZnT3) and vesicular zinc in central nervous system function. Neurosci. Biobehav. Rev. *80*, 329–350.
30. Shatzman, A.R., and Henkin, R.I. (1981). Gustin concentration changes relative to salivary zinc and taste in humans. Proc. Natl. Acad. Sci. USA *78*, 3867–3871.
31. Hershfinkel, M. (2018). The Zinc Sensing Receptor, ZnR/GPR39, in Health and Disease. Int. J. Mol. Sci. *19*, 439.
32. Sunuwar, L., Gilad, D., and Hershfinkel, M. (2017). The zinc sensing receptor, ZnR/GPR39, in health and disease. Front. Biosci. *22*, 1469–1492.
33. Hershfinkel, M. (2023). Cross-talk between zinc and calcium regulates ion transport: A role for the zinc receptor. ZnR/GPR39. J. Physiol. *602*, 1579–1594.
34. Sunuwar, L., Asraf, H., Donowitz, M., Sekler, I., and Hershfinkel, M. (2017). The Zn(2+)-sensing receptor, ZnR/GPR39, upregulates colonocytic Cl(-) absorption, via basolateral KCC1, and reduces fluid loss. Biochim. Biophys. Acta, Mol. Basis Dis. *1863*, 947–960.
35. Chakraborty, M., Asraf, H., Sekler, I., and Hershfinkel, M. (2021). ZnR/GPR39 controls cell migration by orchestrating recruitment of KCC3 into protrusions, re-organization of actin and activation of MMP. Cell Calcium *94*, 102330.
36. Kim, Y.J., Jo, Y., Lee, Y.H., Park, K., Park, H.K., and Choi, S.Y. (2019). Zn(2+) stimulates salivary secretions via metabotropic zinc receptor ZnR/GPR39 in human salivary gland cells. Sci. Rep. *9*, 17648.
37. Asraf, H., Salomon, S., Nevo, A., Sekler, I., Mayer, D., and Hershfinkel, M. (2014). The ZnR/GPR39 interacts with the CaSR to enhance signaling in prostate and salivary epithelia. J. Cell. Physiol. *229*, 868–877.
38. Petersen, O.H. (1986). Calcium-activated potassium channels and fluid secretion by exocrine glands. Am. J. Physiol. *251*, G1–G13.
39. Ambudkar, I. (2018). Calcium signaling defects underlying salivary gland dysfunction. Biochim. Biophys. Acta. Mol. Cell Res. *1865*, 1771–1777.
40. Ahuja, M., Chung, W.Y., Lin, W.Y., McNally, B.A., and Muallem, S. (2020). Ca(2+) Signaling in Exocrine Cells. Cold Spring Harb. Perspect. Biol. *12*, a035279.
41. Horvath, S., Nazmul-Hossain, A.N.M., Pollard, R.P.E., Kroese, F.G.M., Vissink, A., Kallenberg, C.G.M., Spijkervet, F.K.L., Bootsma, H., Michie, S.A., Gorr, S.U., et al. (2012). Systems analysis of primary Sjögren's syndrome pathogenesis in salivary glands identifies shared pathways in human and a mouse model. Arthritis Res. Ther. *14*, R238.
42. Zhang, N., Ji, C., Bao, X., Peng, X., Tang, M., and Yuan, C. (2023). Uncovering potential new biomarkers and immune infiltration characteristics in primary Sjögren's syndrome by integrated bioinformatics analysis. Medicine (Baltim.) *102*, e35534.
43. Bhattacharya, S., Imbery, J.F., Ampem, P.T., and Giovannucci, D.R. (2015). Crosstalk between purinergic receptors and canonical signaling pathways in the mouse salivary gland. Cell Calcium *58*, 589–597.
44. Chorin, E., Vinograd, O., Fleidervish, I., Gilad, D., Herrmann, S., Sekler, I., Aizenman, E., and Hershfinkel, M. (2011). Upregulation of KCC2 activity by zinc-mediated neurotransmission via the mZnR/GPR39 receptor. J. Neurosci. *31*, 12916–12926.
45. Hershfinkel, M., Kandler, K., Knoch, M.E., Dagan-Rabin, M., Aras, M.A., Abramovitch-Dahan, C., Sekler, I., and Aizenman, E. (2009). Intracellular zinc inhibits KCC2 transporter activity. Nat. Neurosci. *12*, 725–727.
46. Sharir, H., and Hershfinkel, M. (2005). The extracellular zinc-sensing receptor mediates intercellular communication by inducing ATP release. Biochem. Biophys. Res. Commun. *332*, 845–852.
47. Garvin, J.L., Burg, M.B., and Knepper, M.A. (1985). Ammonium replaces potassium in supporting sodium transport by the Na-K-ATPase of renal proximal straight tubules. Am. J. Physiol. *249*, F785–F788.
48. Schneditz, G., Elias, J.E., Pagano, E., Zaeem Cader, M., Saveljeva, S., Long, K., Mukhopadhyay, S., Arasteh, M., Lawley, T.D., Dougan, G., et al. (2019). GPR35 promotes glycolysis, proliferation, and oncogenic signaling by engaging with the sodium potassium pump. Sci. Signal. *12*, eaau9048.
49. Moechars, D., Depoortere, I., Moreaux, B., de Smet, B., Goris, I., Hoskens, L., Daneels, G., Kass, S., Ver Donck, L., Peeters, T., and Coulie, B. (2006). Altered gastrointestinal and metabolic function in the GPR39-obestatin receptor-knockout mouse. Gastroenterology *131*, 1131–1141.

50. Khramova, D.S., and Popov, S.V. (2022). A secret of salivary secretions: Multimodal effect of saliva in sensory perception of food. Eur. J. Oral Sci. *130*, e12846.

51. Oka, Y., Butnaru, M., von Buchholtz, L., Ryba, N.J.P., and Zuker, C.S. (2013). High salt recruits aversive taste pathways. Nature *494*, 472–475.

52. Nelson, G., Hoon, M.A., Chandrashekar, J., Zhang, Y., Ryba, N.J., and Zuker, C.S. (2001). Mammalian sweet taste receptors. Cell *106*, 381–390.

53. Shigemura, N., Iwata, S., Yasumatsu, K., Ohkuri, T., Horio, N., Sanematsu, K., Yoshida, R., Margolskee, R.F., and Ninomiya, Y. (2013). Angiotensin II modulates salty and sweet taste sensitivities. J. Neurosci. *33*, 6267–6277.

54. Badahdah, A.A., Al-Ghamdi, S., Banjar, A., Elfirt, E., Almarghlani, A., Elfert, A., and Bahanan, L. (2022). The association between salivary zinc levels and dysgeusia in COVID-19 patients. Eur. Rev. Med. Pharmacol. Sci. *26*, 6885–6891.

55. Goto, T., Komai, M., Suzuki, H., and Furukawa, Y. (2001). Long-term zinc deficiency decreases taste sensitivity in rats. J. Nutr. *131*, 305–310.

56. Kone, B.C., Brady, H.R., and Gullans, S.R. (1989). Coordinated regulation of intracellular K+ in the proximal tubule: Ba2+ blockade down-regulates the Na+,K+-ATPase and up-regulates two K+ permeability pathways. Proc. Natl. Acad. Sci. USA *86*, 6431–6435.

57. Soltoff, S.P., and Mandel, L.J. (1984). Active ion transport in the renal proximal tubule. II. Ionic dependence of the Na pump. J. Gen. Physiol. *84*, 623–642.

58. Koumangoye, R., Bastarache, L., and Delpire, E. (2021). NKCC1: Newly Found as a Human Disease-Causing Ion Transporter. Function (Oxf) *2*, zqaa028.

59. Delpire, E., and Gagnon, K.B. (2018). Na(+) -K(+) -2Cl(-) Cotransporter (NKCC) Physiological Function in Nonpolarized Cells and Transporting Epithelia. Compr. Physiol. *8*, 871–901.

60. Baum, B.J., Afione, S., Chiorini, J.A., Cotrim, A.P., Goldsmith, C.M., and Zheng, C. (2017). Gene Therapy of Salivary Diseases. Methods Mol. Biol. *1537*, 107–123.

61. Kondo, Y., Nakamoto, T., Jaramillo, Y., Choi, S., Catalan, M.A., and Melvin, J.E. (2015). Functional differences in the acinar cells of the murine major salivary glands. J. Dent. Res. *94*, 715–721.

62. Aperia, A., Bertorello, A., and Seri, I. (1987). Dopamine causes inhibition of Na+-K+-ATPase activity in rat proximal convoluted tubule segments. Am. J. Physiol. *252*, F39–F45.

63. Bertorello, A.M., and Katz, A.I. (1993). Short-term regulation of renal Na-K-ATPase activity: physiological relevance and cellular mechanisms. Am. J. Physiol. *265*, F743–F755.

64. Mozaffar, B., Ardavani, A., Muzafar, H., and Idris, I. (2023). The Effectiveness of Zinc Supplementation in Taste Disorder Treatment: A Systematic Review and Meta-Analysis of Randomized Controlled Trials. J. Nutr. Metab. *2023*, 6711071.

65. Yudowski, G.A., Efendiev, R., Pedemonte, C.H., Katz, A.I., Berggren, P.O., and Bertorello, A.M. (2000). Phosphoinositide-3 kinase binds to a proline-rich motif in the Na+, K+-ATPase alpha subunit and regulates its trafficking. Proc. Natl. Acad. Sci. USA *97*, 6556–6561.

66. Benziane, B., and Chibalin, A.V. (2008). Frontiers: skeletal muscle sodium pump regulation: a translocation paradigm. Am. J. Physiol. Endocrinol. Metab. *295*, E553–E558.

67. Lai, L.P., Fan, T.H., Delehanty, J.M., Yatani, A., and Liang, C.S. (1996). Elevated myocardial interstitial norepinephrine concentration contributes to the regulation of Na+,K(+)-ATPase in heart failure. Eur. J. Pharmacol. *309*, 235–241.

68. Huang, X.T., Zheng, Y., Long, G., Peng, W.T., and Wan, Q.Q. (2022). Insulin alleviates LPS-induced ARDS via inhibiting CUL4B-mediated proteasomal degradation and restoring expression level of Na,K-ATPase α1 subunit through elevating HCF-1. Biochem. Biophys. Res. Commun. *611*, 60–67.

69. Saha, P., Manoharan, P., Arthur, S., Sundaram, S., Kekuda, R., and Sundaram, U. (2015). Molecular mechanism of regulation of villus cell Na-K-ATPase in the chronically inflamed mammalian small intestine. Biochim. Biophys. Acta *1848*, 702–711.

70. Paulais, M., and Turner, R.J. (1992). Beta-adrenergic upregulation of the Na(+)-K(+)-2Cl- cotransporter in rat parotid acinar cells. J. Clin. Invest. *89*, 1142–1147.

71. Aperia, A., Ibarra, F., Svensson, L.B., Klee, C., and Greengard, P. (1992). Calcineurin mediates alpha-adrenergic stimulation of Na+,K(+)-ATPase activity in renal tubule cells. Proc. Natl. Acad. Sci. USA *89*, 7394–7397.

72. Ogimoto, G., Yudowski, G.A., Barker, C.J., Köhler, M., Katz, A.I., Féraille, E., Pedemonte, C.H., Berggren, P.O., and Bertorello, A.M. (2000). G protein-coupled receptors regulate Na+,K+-ATPase activity and endocytosis by modulating the recruitment of adaptor protein 2 and clathrin. Proc. Natl. Acad. Sci. USA *97*, 3242–3247.

73. Pedemont, C.H., and Bertorello, A.M. (2001). Short-term regulation of the proximal tubule Na+,K+-ATPase: increased/decreased Na+,K+-ATPase activity mediated by protein kinase C isoforms. J. Bioenerg. Biomembr. *33*, 439–447.

74. Efendiev, R., Bertorello, A.M., and Pedemonte, C.H. (1999). PKC-beta and PKC-zeta mediate opposing effects on proximal tubule Na+,K+-ATPase activity. FEBS Lett. *456*, 45–48.

75. Al-Khalili, L., Kotova, O., Tsuchida, H., Ehrén, I., Féraille, E., Krook, A., and Chibalin, A.V. (2004). ERK1/2 mediates insulin stimulation of Na(+),K(+)-ATPase by phosphorylation of the alpha-subunit in human skeletal muscle cells. J. Biol. Chem. *279*, 25211–25218.

76. Tapella, L., Soda, T., Mapelli, L., Bortolotto, V., Bondi, H., Ruffinatti, F.A., Dematteis, G., Stevano, A., Dionisi, M., Ummarino, S., et al. (2020). Deletion of calcineurin from GFAP-expressing astrocytes impairs excitability of cerebellar and hippocampal neurons through astroglial Na(+)/K(+) ATPase. Glia *68*, 543–560.

77. Almássy, J., Siguenza, E., Skaliczki, M., Matesz, K., Sneyd, J., Yule, D.I., and Nánási, P.P. (2018). New saliva secretion model based on the expression of Na(+)-K(+) pump and K(+) channels in the apical membrane of parotid acinar cells. Pflugers Arch. *470*, 613–621.

78. Gin, E., Crampin, E.J., Brown, D.A., Shuttleworth, T.J., Yule, D.I., and Sneyd, J. (2007). A mathematical model of fluid secretion from a parotid acinar cell. J. Theor. Biol. *248*, 64–80.

79. Sharir, H., Zinger, A., Nevo, A., Sekler, I., and Hershfinkel, M. (2010). Zinc released from injured cells is acting via the Zn2+-sensing receptor, ZnR, to trigger signaling leading to epithelial repair. J. Biol. Chem. *285*, 26097–26106.

80. Anderson, C.T., Radford, R.J., Zastrow, M.L., Zhang, D.Y., Apfel, U.P., Lippard, S.J., and Tzounopoulos, T. (2015). Modulation of extrasynaptic NMDA receptors by synaptic and tonic zinc. Proc. Natl. Acad. Sci. USA *112*, E2705–E2714.

81. Haase, H., and Maret, W. (2005). Fluctuations of cellular, available zinc modulate insulin signaling via inhibition of protein tyrosine phosphatases. J. Trace Elem. Med. Biol. *19*, 37–42.

82. Perez-Rosello, T., Anderson, C.T., Schopfer, F.J., Zhao, Y., Gilad, D., Salvatore, S.R., Freeman, B.A., Hershfinkel, M., Aizenman, E., and Tzounopoulos, T. (2013). Synaptic Zn2+ inhibits neurotransmitter release by promoting endocannabinoid synthesis. J. Neurosci. *33*, 9259–9272.

83. Teixeira, V.L., Katz, A.I., Pedemonte, C.H., and Bertorello, A.M. (2003). Isoform-specific regulation of Na+,K+-ATPase endocytosis and recruitment to the plasma membrane. Ann. N. Y. Acad. Sci. *986*, 587–594.

84. Tremblay, F., Perreault, M., Klaman, L.D., Tobin, J.F., Smith, E., and Gimeno, R.E. (2007). Normal food intake and body weight in mice lacking the G protein-coupled receptor GPR39. Endocrinology *148*, 501–506.

85. Feron, G. (2019). Unstimulated saliva: Background noise in taste molecules. J. Texture Stud. *50*, 6–18.

86. Gaillard, D., and Stratford, J.M. (2016). Measurement of Behavioral Taste Responses in Mice: Two-Bottle Preference, Lickometer, and Conditioned Taste-Aversion Tests. Curr. Protoc. Mouse Biol. *6*, 380–407.

87. Martinez, J.R., and Cassity, N. (1983). Effect of transport inhibitors on secretion by perfused rat submandibular gland. Am. J. Physiol. *245*, G711–G716.

88. Dehpour, A.R., Ghafourifar, P., Juibari, A.M., and Mousavizadeh, K. (1995). Alteration by ouabain of rat submandibular glands function. Gen. Pharmacol. *26*, 1009–1013.

89. Martínez, J.R. (1971). Action of ouabain on submaxillary secretion in the dog. J. Pharmacol. Exp. Ther. *178*, 616–624.

90. Oliveira, R.D., Navas, H., Durán, C., Pinto, M., Gutiérrez, J., and Eblen-Zajjur, A. (2013). Salivary [Na+], [K+] and [Cl-] changes induced by combined treatment with Na/K ATPase (digoxine) and Na/K/2C1 (furosemide) inhibitors in congestive heart failure patients. Curr. Top. Pharmacol. *17*, 79–83.

91. Loper, H.B., La Sala, M., Dotson, C., and Steinle, N. (2015). Taste perception, associated hormonal modulation, and nutrient intake. Nutr. Rev. *73*, 83–91.

92. Rhodus, N.L., and Brown, J. (1990). The association of xerostomia and inadequate intake in older adults. J. Am. Diet Assoc. *90*, 1688–1692.

93. Jin, H., Fishman, Z.H., Ye, M., Wang, L., and Zuker, C.S. (2021). Top-Down Control of Sweet and Bitter Taste in the Mammalian Brain. Cell *184*, 257–271.e16.

94. Li, M., Tan, H.E., Lu, Z., Tsang, K.S., Chung, A.J., and Zuker, C.S. (2022). Gut-brain circuits for fat preference. Nature *610*, 722–730.

95. Gilad, D., Shorer, S., Ketzef, M., Friedman, A., Sekler, I., Aizenman, E., and Hershfinkel, M. (2015). Homeostatic regulation of KCC2 activity by the zinc receptor mZnR/GPR39 during seizures. Neurobiol. Dis. *81*, 4–13.

96. Evans, G.W. (1986). Zinc and its deficiency diseases. Clin. Physiol. Biochem. *4*, 94–98.

97. Tsuchiya, H. (2022). Gustatory and Saliva Secretory Dysfunctions in COVID-19 Patients with Zinc Deficiency. Life *12*, 353.

98. Toan, N.K., and Ahn, S.G. (2021). Aging-Related Metabolic Dysfunction in the Salivary Gland: A Review of the Literature. Int. J. Mol. Sci. *22*, 5835.

99. Aliani, M., Udenigwe, C.C., Girgih, A.T., Pownall, T.L., Bugera, J.L., and Eskin, M.N.A. (2013). Zinc deficiency and taste perception in the elderly. Crit. Rev. Food Sci. Nutr. *53*, 245–250.

100. Su, J.C., and Birmingham, C.L. (2002). Zinc supplementation in the treatment of anorexia nervosa. Eat. Weight Disord. *7*, 20–22.

101. Yagi, T., Asakawa, A., Ueda, H., Ikeda, S., Miyawaki, S., and Inui, A. (2013). The role of zinc in the treatment of taste disorders. Recent Pat. Food, Nutr. Agric. *5*, 44–51.

102. Shintani, T., Ohta, K., Ando, T., Hayashido, Y., Yanamoto, S., Kajiya, M., and Shiba, H. (2023). Retrospective study on the therapeutic efficacy of zinc acetate hydrate administration to patients with hypozincemia-induced dysgeusia. BMC Oral Health *23*, 159.

103. Figueroa, J.A.L., Stiner, C.A., Radzyukevich, T.L., and Heiny, J.A. (2016). Metal ion transport quantified by ICP-MS in intact cells. Sci. Rep. *6*, 20551.

104. Chandrashekar, J., Kuhn, C., Oka, Y., Yarmolinsky, D.A., Hummler, E., Ryba, N.J.P., and Zuker, C.S. (2010). The cells and peripheral representation of sodium taste in mice. Nature *464*, 297–301.

105. Yiannakas, A., Kolatt Chandran, S., Kayyal, H., Gould, N., Khamaisy, M., and Rosenblum, K. (2021). Parvalbumin interneuron inhibition onto anterior insula neurons projecting to the basolateral amygdala drives aversive taste memory retrieval. Curr. Biol. *31*, 2770–2784.e6.

STAR★METHODS

KEY RESOURCES TABLE

REAGENT or RESOURCE	RESOURCE SOURCE	IDENTIFIER
Chemicals, peptides, and recombinant proteins		
Dulbecco′s Modified Eagle′s Medium (DMEM)	Biological Industries	01-055-1A
Fetal Calf Serum	Biological Industries	04-001-1A
pen-strep	Biological Industries	03-031-1B
L-Glutamine	Biological Industries	03-020-1B
Zinc sulfate heptahydrate	Sigma- Aldrich	z4750
Ammonium chloride	Sigma- Aldrich	A9434
Sodium chloride	Sisco Research Laboratories	41721
Sacarine	Sigma- Aldrich	56047
Rubidium chloride	Sigma- Aldrich	R2252
Hydrogen Peroxide	Fisher Chemical	H/1820/15
Nitric acid	Sigma- Aldrich	225711
RNA later solution	Invitrogen	AM7020
BCECF-AM	Tef Labs	Not available
siGPR39	5′-CCAUGGAGUUCUACAGCAU-3′	Integrated DNA Technologies, IDT
siNA/K pump α1 subunit	5′-CAUGAAGCUGAUACGACAGAGAATC-3′	Integrated DNA Technologies, IDT
SCR	5′- GCCCAGAUCCCUGUACGU-3′	Integrated DNA Technologies, IDT
*Trans*IT-X2	mirusbio	MIR 6000
DIOA 2-[(2-butyl-6,7-dichloro-2-cyclopentyl-1-oxo-3H-inden-5-yl)oxy]acetic acid	Sigma-Aldrich	D129
Bumetanide 3-(butylamino)-4-phenoxy-5-sulfamoylbenzoic acid	Sigma-Aldrich	B3023
YM-254890	FUJIFILM Wako Pure Chemical Corporation	257-00631
Ouabain	Sigma-Aldrich	O3125
FK506	InvivoGen	inh-fk5-5
Tetraethylammonium chloride	Sigma-Aldrich	T2265
Harris Hematoxylin Solution	Sigma-Aldrich	HHS32
Eosin alcoholic solution	kaltek	1120
Antibodies		
Anti Na/K ATPase pump α1 subunit	Abcam	Ab7671; RRID:AB_306023
Dapi-containing immunomount	SouthernBiotech	0100-20
Critical commercial assays		
PureLink™ RNA Mini Kit	Invitrogene	12183018a
cDNA synthesis kit	Quanta bio	95047
qPCR bio probe blue mix	PCR biosystem	pb20.25-05
Experimental models: Cell lines		
CVCL_B032	Our collection	HSY
CRL-1573	ATCC	HEK293
Experimental models: Organisms		
GPR39$^{-/-}$ and GPR39$^{+/+}$ C57BL6/RCC	*Oue line*, mice bred in our facility	GPR39tm1Lex

EXPERIMENTAL MODEL AND STUDY PARTICIPANT DETAILS

All experimental procedures performed on animals were done in accordance with a protocol approved by the committee for Ethical Care and Use of Animals in Research at the Faculty of Health Sciences at Ben-Gurion University of the Negev, approval number: IL51-06-2023B. Mice, GPR39$^{-/-}$ and GPR39$^{+/+}$ C57BL6[49] were bred in our animal facility. Male mice ages 12-16 weeks were used for tissue preparation used for imaging or for behavioral experiments.

For *in vitro* analysis of ZnR/GPR39 the human salivary gland cell line, HSY and HEK 293 cells was grown in Dulbecco's Modified Eagle's Medium (DMEM, Biological Industries, Israel) supplemented with 10% (v/v) fetal calf serum (Biological Industries, Israel) and 1% pen-strep solution, 1% L-glutamine, grown in 5% CO_2 humidified atmosphere at 37°C.

METHOD DETAILS

For gene-silencing experiments, cells were transfected with siRNA constructs aimed to silence the Na^+/K^+ ATPase pump or a scrambled (si-control) siRNA construct (40 nM, Sigma-Aldrich) in 60mm plates, using the Mirus transfection reagent as described by the manufacturer (Fisher scientific). Cells were imaged or used for qPCR analysis 48 hours after transfection. The target sequence of the Na^+/K^+ ATPase pump for siRNA was: sense 5′ CAUGAAGCUGAUACGACAGAGAATC, anti-sense: 5′AGGUACUUCGACU AUGCU GUCUCUUAG. The target sequence of the siControl for siRNA was: sense 5′GCCCAGATCCCTGTACGTtt, anti-sense 5′ ACGTACAGGGATCTGGGCtt.

For overexpression of ZnR/GPR39 and the Na^+/K^+ ATPase pump in HEK293 cells, cells were transfected with plasmids of pcDNA, GPR39 (pCMV6-Entry) and Na^+/K^+ ATPase pump α1 (RC201009) and β1 (RC200500) in 60 mm plates using the Mirus reagent as above. Cells were loaded with BCECF and imaged 48 hours after transfection.

Expression of Na^+/K^+ ATPase pump or GPR39 was determined in HSY cells. Cells were seeded on 60 mm plates, after 48 hours cells are trypsinized with 0.25% trypsin (Biological Industries). Cell lysates were homogenized using QIA10 shredder, as described by the manufacturer (QIAGEN). Total RNA was purified using RNeasy Mini Kit as described by the manufacturer (QIAGEN). 1μg RNA was converted to cDNA using Verso cDNA synthesis kit as described by the manufacturer (Thermo Scientific). cDNA is diluted 1:5 (as per calibration) with ultrapure water and subjected to PCR cycles (BIOER). Primers and probes were supplied by IDT by the following sequences: Na^+/K^+ ATPase: forward primer-CACACCTTTGGCAATAGCTTT, reverse primer-CTCCATGATTGACCCTCCAC. GPR39: forward primer- CAGGAGGCAGACCATCATC reverse primer- CTCGTCCAGTCGTGCTTG.

Expression of Na^+/K^+ ATPase pump was determined from salivary glands tissue. Tissue was extracted from anesthetized mice and kept in RNA later solution (Invitrogen) for 24 hours. RNA purification was done using MACHEREY-NAGEL RNA extraction kit. 1μg RNA was converted to cDNA using Verso cDNA synthesis kit as described by the manufacturer (Thermo Scientific). cDNA was diluted 1:5 (as per calibration) and subjected to PCR cycles (BIOER). Primers were supplied by IDT by the following sequences: Na^+/K^+ ATPase: forward primer- CTTCTCTTTCTAGTCTCCAGCA, reverse primer- TTGTCACCATGCTCCGATAC.

Rb^+ uptake assay

Ouabain-sensitive rubidium (Rb^+) uptake was used to monitor K^+ transport activity, as previously done.[48] Following brief Zn^{2+} (200μM, 2 minutes) treatment to activate ZnR/GPR39, without inducing Zn^{2+} permeation, cells were incubated with Rb^+ in the presence or absence of ouabain. Previous studies showed that trace amounts of Rb^+ (4.7mM) present better signal to noise ratio,[48,103] we therefore used these trace concentrations. Cell lysates were used for spectroscopic analysis of Rb^+, using ICP-OES (5100-Agilent, 780.026nm wavelength) and compared to a calibration solution to determine concentrations of Rb^+ in the cells.

Fluorescent imaging

Cells grown on coverslips were loaded at room temperature with 1 μM 2′,7′-Bis(2-carboxyethyl)-5(6)-carboxyfluorescein (BCECF-AM, 10 minutes, Tef Labs) in Ringer's solution composed of (in mM): 120 NaCl; 5.4 KCl; 1.8 $CaCl_2$; 0.8 $MgCl_2$; 10 HEPES; 10 glucose; pH 7.4. Cells were then washed in Ringer's solution and incubated for an additional 15 minutes at room temperature. Coverslips were then mounted in a perfusion chamber of a Zeiss Axiovert 200 microscope and images were acquired every 3 s (Indec Imaging Workbench 5) using a 10× objective with 4 × 4 binning of the image (Sensi-Cam, PCO). BCECF was excited at 440 nm and 470 nm with polychrome monochromator (TILL Photonics), and imaged with a 510-nm long-pass filter. The fluorescent signal is presented as the ratio between the two wavelengths (R = F440/F470). All results shown are traces of the averaged responses of at least 20-30 cells in each experimental paradigm, for each condition at least 3 independent experiments.

NH_4Cl paradigm for monitoring K^+ transport

Cells/acute slices loaded with a pH-sensitive dye, BCECF, were used to study ion transport activity.[35,44] Following application of NH_4Cl, which is found in equilibrium of NH_4^+/NH_3 in the perfusing Ringer's solution, we observed initial alkalization that is induced by NH_3 diffusion into the cytoplasm. Subsequently, activation of ion transport systems and transport of NH_4^+, as a surrogate to K^+,[47,70] is expected to acidify the cytoplasm and lead to a decrease in BCECF fluorescence. Treatment with extracellular Zn^{2+} (200μM) or inhibitors was done immediately prior to imaging, as indicated for each experiment. Cells/acute slices were perfused with K^+-free Ringer's solution to obtain baseline fluorescence, which was then exchanged to K^+-free Ringer's solution that included

10mM NH_4Cl for cells or 20mM of NH_4Cl for acute slices, while monitoring BCECF fluorescence. The rate of acidification, representing K^+ transport rate, was determined using a linear fit obtained during a 50 or 100s period (as indicated in legend) following the peak fluorescence signal.

Animals

All experimental procedures performed on animals were done in accordance with a protocol approved by the committee for Ethical Care and Use of Animals in Research at the Faculty of Health Sciences at Ben-Gurion University of the Negev, approval number: IL51-06-2023B. Briefly, mice were housed in specific pathogen-free facilities. Rodent care practices were maintained under sterile conditions, with sterile supplies. Rodent husbandry conditions were 12:12 light:dark cycles at 20–24°C and 30–70% relative humidity. Animals were free-fed autoclaved rodent chow and had free access to reverse-osmosis filtered water. Rodents were housed in individually ventilated GM500 (Tecniplast, Italy) cages in groups of maximum five mice per cage. Male mice ages 12-16 weeks were used for tissue preparation for imaging or for behavioral experiments. Mice were sacrificed by isoflurane according to the protocol. For genotyping, mice tail biopsy samples were incubated for 30 minutes at 95°C in 180μl lysis buffer containing: 25mM NaOH and 0.2mM EDTA to isolate the DNA. Lysates were maintained at room temperature for 5 minutes and neutralized by adding 180μl of 40mM Tris base solution. Following the PCR amplification, samples were loaded on Sybr gold (Invitrogen, USA) containing agarose gel for electrophoresis. Genetic background of ZnR/GPR39 WT and knockout animals was determined by multiplex polymerase chain reaction (PCR), that was performed using the primers 5'-AACAGCGTCACCATCAGGGTT-'3 and 5'-TGCGAGAGAGGTTGC AGTTGA-'3 (Integrated DNA Technologies, IDT) for WT allele that amplified a 445 bp band, and the second primer set for KO allele 5'-GGAACTCTCACTCGACCTGGG-'3/5'-GCAGCGCATCGCCTTCTATC-'3 (IDT) that amplified a 262 bp band. PCR reactions were performed with Red Mix (LAROVA GmbH) solution according to the manufacturer's protocol.

Tissue preparation for live fluorescence imaging

Male mice (12-14 weeks old) were anesthetized with Ketamine/Xylazine and then the salivary glands were exposed by an incision along the neck and the glands were extracted into ice cold slice saline buffered solution.[61] Acute slices were taken from the submandibular (SMG) or parotid glands, and kept in slice saline solution containing: 140mM NaCl, 5mM KCl, 1mM MgCl, 10mM glucose, 0.8mM thiourea, 0.4mM ascorbic acid, 10mM Na-Hepes (pH 7). The slices were loaded with BCECF-AM in the presence of 0.02% Pluronic acid, dissolved in slice solution for 30 minutes on room temperature. Excess dye was washed by incubating the slices in fresh slice solution for additional 10 minutes at room temperature, after which the slices were transferred to the recording chamber and mounted on the imaging microscope and NH_4Cl paradigm (see above) was performed. This paradigm was similarly used to show K^+-dependent transport activity in parotid glands,[70] as well as Na^+/K^+ ATPase activity.[47] Live tissue imaging was performed on an Olympus (IX-50) microscope with a 10X water-immersed objective connected with Polychrome IV monochromator (TILL Photonics, Germany) and fluorescence changes were recorded with SensiCam cooled charge-coupled camera (PCO, Germany) and measured with Imaging Workbench 5 (Indec, CA).

Immunofluorescent histological analysis of salivary gland tissue sections

Following the Ketamine/Xylazine cocktail anesthesia, 3-month-old C57bl/6 mice were transcardially perfused with ice-cold PBS and 4% paraformaldehyde. Glands were extracted and postfixed in same fixative overnight at 4°C. Tissue was then washed with PBS, dehydrated with increasing series of ethanols and infiltrated with paraffin. 7μm paraffin sections were obtained on a rotary microtome. After heat-induced antigen retrieval in 10mM sodium citrate (at 95°C for 10 minutes), tissue sections were washed 3 times (5 minutes each) in PBS and then blocked with 5% normal goat (NGS), 0.1% Triton in PBS (blocking solution). Sections were incubated with mouse anti- α1 subunit of Na^+/K^+ ATPase primary antibody (Abcam, ab7671) overnight at 4°C. Next day, sections were washed with PBS three times (5 minutes each) and incubated with Alexa594 conjugated goat anti-mouse for 1 hour at room temperature. For all immunofluorescent labeling experiments, sections were washed with 1X PBS and mounted using a Dapi-containing immunomount to mark nuclei. Tissues were then imaged using Nikon C2 confocal microscope and image analysis was done using ImageJ.

Salivary secretion measurements

3-months old male mice were used, and food was removed overnight before the saliva collection.[51,104] Mice were anesthetized with Ketamine/Xylazine cocktail and pilocarpine (10 mg/kg) was injected. Saliva was collected for 15 min, using an apparatus as described previously,[60] and weighed to determine salivary secretion. For ion measurements, saliva was stored in 4°C for overnight. Saliva samples were analyzed using potentiometery and routine protocols in the biochemistry lab in Soroka Medical hospital, Israel, and the samples were measured for Na^+, K^+ and Cl^- ions content. Zinc levels were measured in fresh saliva samples using ICP-OES using axial configuration at wavelengths of 202nm, 206nm and 213nm.

Taste acuity measurements

Prior to the test, 2 bottles of water were given to the mice for 24 hours. Mice were water deprived for 18 hours before performing the taste testing.[105] For the test, one bottle contained water and the other contained the tastant as previously done.[51,52,105] Different concentration of tastant, as indicated, were presented to the mice in each experimental session and the amount of liquid that remained in the bottle was measured after 24 hours of exposure to the bottles. Water/tastant bottles were switched after 24 hours and the amount

drank was measured again. The results are presented as the amount of tastant consumed during a 24 hours period by a mouse, out of the total amount drank. If more than 50%, the mice preference to the tastant was higher than chance, and vice versa.

QUANTIFICATION AND STATISTICAL ANALYSIS

Each column scatter plot represents all (n) values, and the calculated average of measurements from at least three independent experiments. Statistical analysis was performed using unpaired Two-tailed Student's t-test, comparing each treatment to Zn^{2+} treatment of cells or tissues under the same conditions (control, silencing with empty vectors or treatment with solvents when inhibitors were applied), as marked in the legends. A p value of less than 0.05 ($p < 0.05$) was considered statistically significant. N.S non- significant, * $p < 0.05$; ** $p < 0.01$; *** $p < 0.001$.

Generalized data: not relevant.